Hindawi Publishing Corporation
Journal of Sensors
Volume 2015, Article ID 984627, 6 pages
http://dx.doi.org/10.1155/2015/984627

Research Article

Sensing of Tooth Microleakage Based on Dental Optical Coherence Tomography

Chia-Wei Sun,[1] Yi-Ching Ho,[2,3] and Shyh-Yuan Lee[2,4]

[1]*Biomedical Optical Imaging Lab, Department of Photonics, National Chiao Tung University, Hsinchu, Taiwan*
[2]*School of Dentistry, National Yang-Ming University, Taipei, Taiwan*
[3]*Department of Dentistry, National Yang-Ming University Hospital, Yilan, Taiwan*
[4]*Department of Stomatology, Taipei Veterans General Hospital, Taipei, Taiwan*

Correspondence should be addressed to Chia-Wei Sun; chiaweisun@nctu.edu.tw

Received 29 July 2014; Accepted 7 November 2014

Academic Editor: Jui-che Tsai

This study describes microleakage sensing based on swept-source optical coherence tomography (SS-OCT). With a handheld scanning probe, the SS-OCT system can provide portable real-time imaging for clinical diagnosis. Radiography is the traditional clinical imaging instrument used for dentistry; however, it does not provide good contrast images between filling material and the enamel of treated teeth with microleakage. The results of this study show that microleakage can be detected with oral probing using SS-OCT *in vivo*. The calculated microleakage length was 401 μm and the width is 148 μm, which is consistent with the related histological biopsy measurements. The diagnosis of microleakage in teeth could be useful for prevention of secondary caries in the clinical treatment plans developed in the field of oral medicine.

1. Introduction

The oral cavity consists of three main parts: (1) hard tissue, including tooth and alveolar bone, (2) soft tissue, including mucosa and gingiva tissues, and (3) periodontal tissues. Caries might be the most frequently encountered problem because of its high prevalence and wide distribution among all ages. The World Health Organization (WHO) reported that dental caries continues to be a major public health problem globally and a major public health problem in most high-income countries; in 2009, this disease affected 60–90% of school aged children and the vast majority of adults [1]. In addition, dental caries has shown certain correlations with a variety of systemic diseases such as systemic infections, kidney inflammation, and septicemia [2–5]. For treating carious tooth, dentists remove sections with a lesion and fill the area with restoration materials. Root canal treatment is needed for teeth that have deep caries involving pulp and irreversible pulpitis. However, no matter what treatment is used, patients are at risk for secondary caries. The Federation Dentaire Internationale defines secondary caries as positively diagnosed carious lesions that occur at the margins of an existing restoration [6]. This is an important clinical problem; it reduces the lifetime of dental restorations, alters dental hard tissue, and endangers tooth survival [7]. It is difficult to diagnose secondary caries during the early stages where survival of the tooth and crown restoration is most likely.

One of the main causes of secondary caries is microleakage. Microleakage means the "gap" between tooth and restorative materials [8–10]. Rodrigues et al. demonstrated the microleakage beneath composite resin restorative material [10].

Food debris and dental plaque may stick to these undersized gaps and consequently lead to secondary caries. In general, patients cannot adequately clean these tiny sites. In addition, the detection of microleakage is very difficult for the dentist in most clinical settings. Traditionally, the diagnosis of these problems has been based on clinical examination with dental probes and radiographs. The poor reliability and reproducibility of dental probes may cause misdiagnosis because of the difficulty with localization of gaps. For microleakage, most of bonding agents are not radiopaque and there would be no distinction between the adhesive resin and the microleakage in an X-ray radiograph/tomogram.

Therefore, it is more difficult to diagnose where the microleakages are compared to cracks. Furthermore, radiography measurements are accompanied by radiation exposure. Although there are many new methods for diagnosis under development in the laboratory [11–13], these methods are only applied when secondary caries already exists.

Optical coherence tomography (OCT) may provide a good tool for the diagnosis of microleakage [14]. OCT was first reported by Huang et al. [11] in 1991 and has been widely used in numerous clinical applications, including gastroenterology [16], ophthalmology [17], dermatology [18], and dentistry [19, 20]. In dental science, OCT detects qualitative and quantitative morphological changes of dental hard and soft tissues *in vivo*. Furthermore, OCT can also be used for early diagnosis of dental diseases, including caries, periodontal disease, and oral cancer, because of the excellent spatial resolution. The first *in vitro* images of dental hard and soft tissues in a porcine model were reported in 1998 [21]. Later, the *in vivo* imaging of human dental tissue was presented [9]. Early detection and treatment can increase the survival rates of teeth and patients. Three-dimensional imaging ability is another advantage of dental OCT. It helps clinicians to locate problems in soft and hard tissues more accurately and rapidly. Table 1 shows a comparison of the methods used in general dentistry for diagnosis currently. Compared with these methods, OCT can provide effective information because it is noninvasive and nondestructive and does not expose patients to radiation; in addition, it provides a real-time monitoring method. The swept-source optical coherence tomography (SS-OCT) has more benefits compared to conventional time domain (TD) and Fourier domain (FD) OCT including imaging speed, detection efficiency, sensitivity, simpler system setup, and better signal-to-noise ratio (SNR) with suitable filter [22–24]. The SS-OCT has high axial resolution of about 10 μm [22]; this allows sufficient information for dental clinical applications such as the diagnosis of crack and microleakage detection. The aim of this study was to provide preliminary information for the diagnosis of microleakage to prevent advanced secondary caries based on SS-OCT *in vivo* using a fiber optic handheld scanning probe. The microleakage identified, between composite resin and enamel, was quantified using the OCT image. Clinicians can provide more appropriate dental treatment that prevents secondary caries with the diagnosis made according to the information provided by handheld probe SS-OCT.

Table 1: Comparison of secondary caries detection methods.

Methods	Type	Descriptions
Radiography [18–20]	*In vivo*	(1) Limited spatial resolution (2) Radioactive
Dental probe [21]	*In vivo*	(1) Limited spatial resolution (2) No image
Dental computed tomography [9]	*In vivo*	(1) Limited spatial resolution (2) Radioactive (3) Expensive
Laser fluorescence spectrometer [22, 23]	*In vitro*	(1) *In vitro* experiment (2) Biomarker is necessary
SS-OCT [17]	*In vivo*	(1) High space resolution (2) Real-time images (3) Nonradioactive (4) Dental probe was developed (5) 3D image reconstruction is available

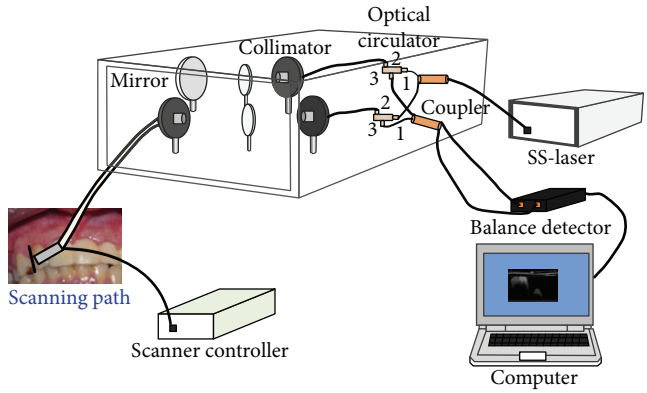

Figure 1: Setup of the dental OCT. The incident light separates into two arms (reference arm and sampling arm) and is recoupled in another optical coupler for interference. A balance detector is used for the reduction of noise and then a DAQ card receives the signal.

2. Materials and Methods

2.1. System Setup. An SS-OCT system with a handheld scanner probe is built with a 1310 nm swept-source laser (Santec, HSL-2100) as a broadband light source. Figure 1 shows the OCT scheme. The main passive components are integrated into a metal case. The fiber-based Mach-Zehnder interferometer includes couplers and two optical circulators. The balance detector is used for interference detection, and the data acquisition card (DAQ card, NI-PCI 5122) provides computer-photodetector interfacing. The wavelength-scanning rate is 20 kHz. The frame rate is 20 Hz (1000 A-scans/frame). The electric signal acquisition rate is 100 MS/s by NI-PCI 5122. Experimental data were collected and analyzed using LabVIEW (National Instrument) software. Figure 2 shows the handheld probe used with a 3 mm outer diameter. The probe was connected to the sampling arm of the OCT with fiber and driven by individual mechanics. The weight of this probe is less than 150 grams. A reflection mirror is placed on the shaft of the turbine which provides the optical scanning. The quartz glass is used as the optical window. Gas is injected from the needle which is inserted to hole of the shaft bearing. An optical focuser is mounted in the center of the tube. The body of the catheter is made from polytetrafluoroethylene (PTFE) tube. Including the glue used in the catheter, the entire sheath is made from biocompatible material. The integrated SS-OCT system offers excellent portability and is easy to operate for patients with

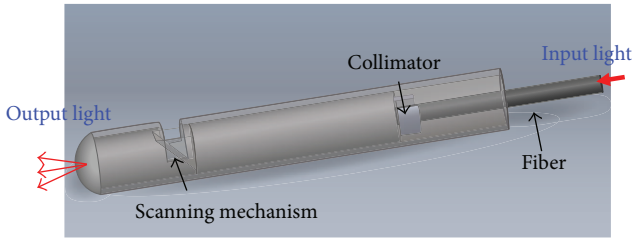

Figure 2: The portable dental OCT probe. The light inputs a fiber-based probe and is focused by a collimator. An electoral scanning mechanism changes the output light angle and a scanning path is realized.

disabilities, the elderly, and children. For good infection control, a disposable PTFE cover is attached to this intraoral probe for clinical experiments.

2.2. In Vivo Measurement. A volunteer that had maxillary right lateral incisor and maxillary right first premolar treated for caries and four artificial temporary composite resin crowns of maxillary right central incisor and maxillary left central incisor was enrolled in the study. Figure 3(a) shows an intraoral photograph. The distal caries of maxillary right first premolar was treated and restored with composite resin two days before the study. The teeth were brushed before the experiment to avoid the effects of debris. Using a similar color scheme, the composite resin is difficult to distinguish from sound tissue in the photograph, Figure 3(a). Figure 3(b) is a radiograph of sample teeth. The radiopaque images of the treated area with composite resin can be seen in the radiograph. Because of the space resolution limitation of the radiograph, the microstructures, including the treated tooth surface, cannot be observed in this image. It is difficult to diagnose a microleakage using a dental probe and radiographs. The institutional review board (IRB) permission number is 100104 from National Yang-Ming University, Taipei, Taiwan.

2.3. Experimental Method. Using radiographs and clinical examination, the regions of interest were chosen and marked for OCT imaging. The scanning probe acquired images on the marked tooth. A metal marker was placed on the probe to ensure complete image acquisition at each rotating scan the metal has high reflection on the OCT image. The detected light is stable for good image quality with a range of angle. In addition to the treated tooth, the sound tooth and the artificial composite resin crown, of the same patient, were also measured to obtain a standard sample. The results are shown in Figures 4, 5, and 7, at 6 mm × 4 mm. The tooth location numbers are marked in the brackets under each figure.

3. OCT Imaging Results

Figure 4 shows the OCT images of a sound tooth. The tooth structure and gingiva are noted and identified in these images. The tooth cervical area under the gingiva can also be observed. These findings indicated that the OCT system worked with regard to tooth imaging. The probe marker

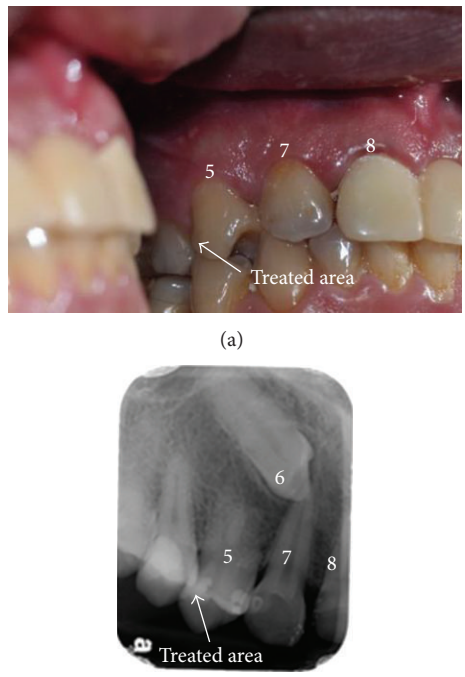

Figure 3: (a) A photograph and (b) the radiograph of the volunteer's tooth 8: maxillary right central incisor; 7: maxillary right lateral incisor; 6: impacted maxillary right canine; 5: maxillary right first premolar. The distal caries of maxillary right first premolar (5) was treated and restored with composite resin two days before the study.

image can be seen at the top of the image. The side effects were removed and compensated for in follow-up images. Figures 4(b) and 4(c) show the treated tooth with and without a gap between the composite resin and enamel. In Figure 4(b), the composite resin was completely attached to the enamel sides and there was no microleakage observed. These findings suggest that the treated teeth had almost no risk of secondary caries. Figure 4(c) shows the same treatment condition with microleakage between the composite resin and enamel on the left side. This microleakage was less than 1 mm and difficult to see by photography and radiography. When dental plaque is stuck in such a gap, there is a very high risk of secondary caries. Such conditions reduce the lifetime of artificial crowns. Figure 5 shows the artificial composite resin crown and a sound tooth by OCT related to Figure 4 after all imaging.

4. Microleakage Detection

Although Figures 4(c) and 5(c) show the locations of microleakage, further information, such as calculation of the dimensions, is important for the clinical diagnosis. Figure 6 is a flowchart of the imaging process. The first step was removal of the unnecessary image with the top probe marker. Compensating for distortion that came from the scanning vibration was the next step. As illustrated in Figure 4, this affects the OCT images visibly and may result in mistakes

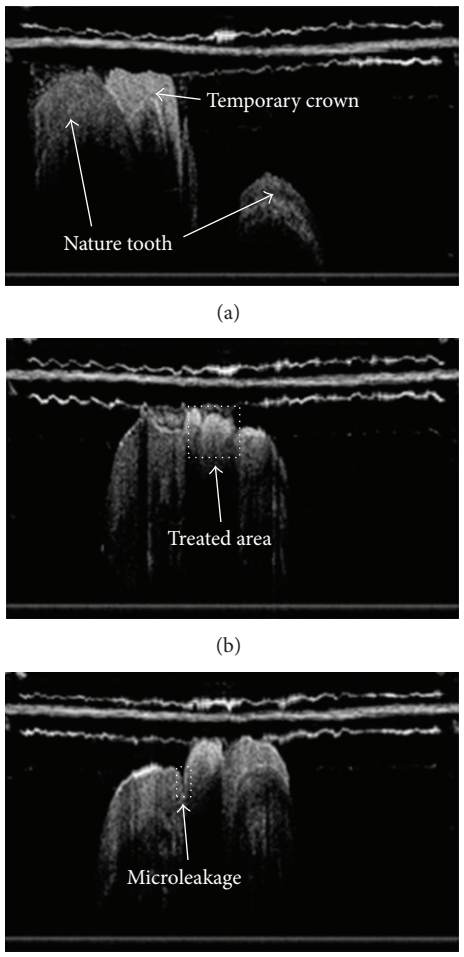

Figure 4: The treated tooth, OCT images: (a) composite resin and natural tooth; (b) treated tooth without microleakage; (c) treated tooth with microleakage.

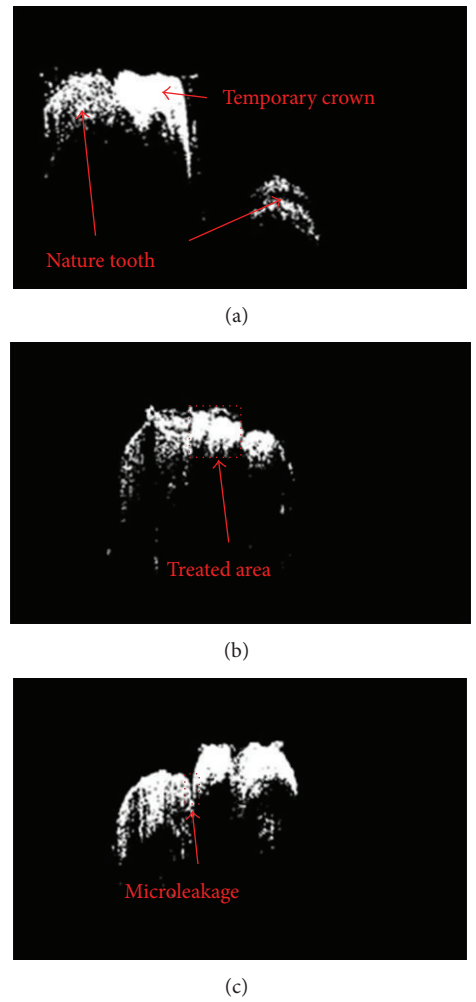

Figure 5: The treated tooth OCT images of Figure 4 after image processing: (a) composite resin and natural.

when calculating the microleakage dimensions. An average line for the marker image was used for compensation. After observing the difference between this line and the OCT image, the necessary calculation for the pixel number of each column was obtained. Hence, the compensation images could be redrawn. Then, image binarization and the filtered edges were used to calculate the dimension of the microleakage.

Different from the human tooth, dentin porosity properties were observed in the organic tubules. Composite resin is a compound with ultraviolet characteristics. It was inseparable from and indicated by a bright area next to a natural tooth in the processed OCT images. A dentist can examine the composite resin areas of treated enamel on these images. The OCT image can help clinicians locate and assess the treated part rapidly. For a detailed diagnosis, the area of interest on the OCT image can be evaluated, for example, the microleakage, for advanced calculation. Figure 7(a) shows an enlarged microleakage area chosen from Figure 5(c). The area of interest was chosen and resized. An edge filter was then used for observation of the image boundary. The width and depth of the microleakage could be calculated using a very simple formula, shown in

$$w = \frac{6n_x}{m_x}, \qquad d = \frac{2n_y}{m_y}, \tag{1}$$

where w and d were the calculated width and depth and n and m were the counted t pixel numbers and the pixel numbers for the whole OCT image on the x-axis (width) and the y-axis (depth). The constant coefficients, 6 and 2, showed the physical dimensions of the measurement area to be 6 mm × 2 mm. In this study, the pixel numbers of each image were 960 × 500. Therefore, the calculated microleakage length was 401 μm and the width was 148 μm. This result was very close to the clinical results and indicated that the system used had good spatial resolution when compared to traditional tools. For clinical diagnosis, the OCT image provides accurate information for the assessment of microleakage. The microleakage region can be assessed with this processing.

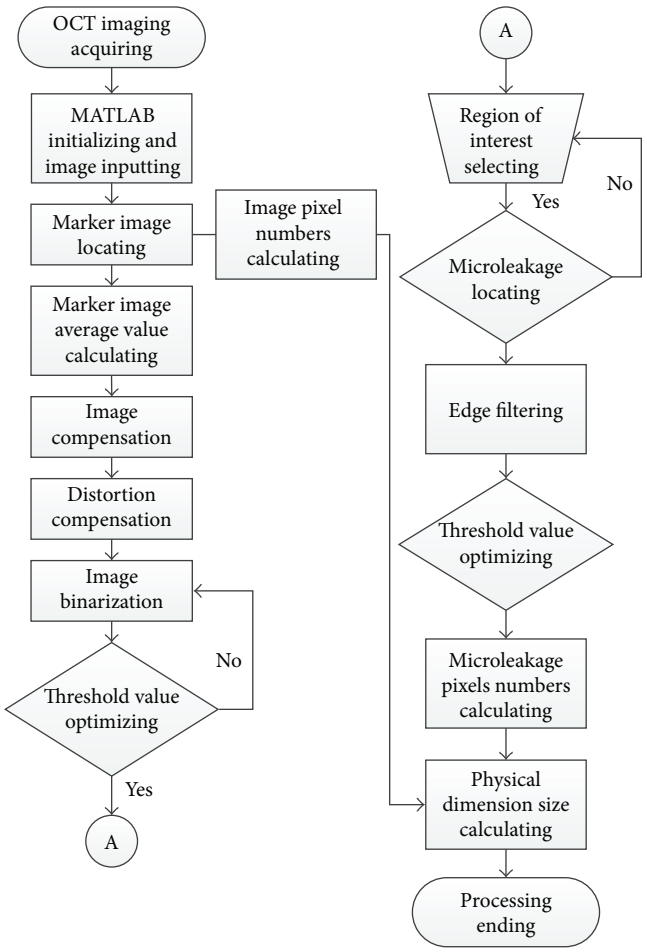

Figure 6: Flowchart of the OCT imaging process.

As referenced in a prior report [16], the boundary of the microleakage can be marked in red for clinician focus.

5. Discussions

In this study, we observed the treated area several times and similar results were obtained. Therefore, we believe the results are still significant because of the consistency of OCT images. Of course, some issues still should be considered in follow-on works.

First, the microleakage between tooth and composite resin was obtained by OCT system. However, there are many dental filling materials such as amalgam and glass ionomer (GI) that were also widely used in endodontics. Therefore, experiments with different filling materials should be carried out because of those different image properties such as penetration depth and image distortion and the minimum detectable gap size will be obtained. Second, variety of tooth surfaces such as buccal, lingual surfaces, and interproximal should also be measured. The restorations measurement at the gingival margins is also necessary because of the fact that microleakage and secondary caries are especially problematic at these areas. These issues will be considered in the future works.

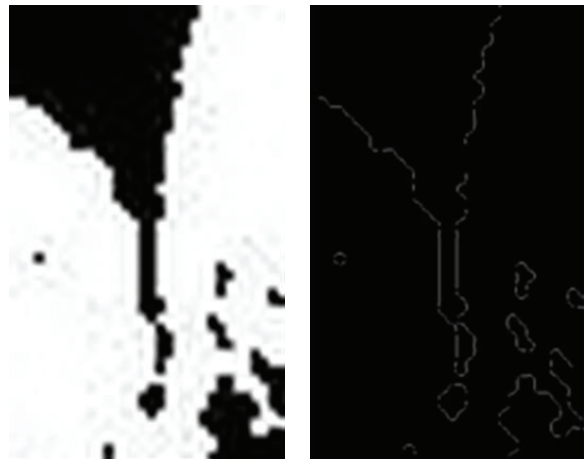

(a) (b)

Figure 7: Processed gap part for gap detection: (a) binarization processed tooth gap image and (b) gap boundary.

6. Conclusion

The results of this research showed that SS-OCT could be used for the detection of cracks in the enamel of teeth [24]. SS-OCT was very reliable for the diagnosis of cracks. However, this study provided *ex vivo* information for large crack detection only. Different to microleakage, the crack raises a rare chance for secondary caries. As mentioned in previous section, the main reason of secondary caries is the accumulated bacteria from food debris or plaque stuck in microleakages. In our study, the diagnosis of *in vivo* microleakage can be achieved by using a portable SS-OCT with dental probe measurement. A handheld scanning probe was integrated into a portable SS-OCT system. Clinicians can detect the microleakages *in vivo*, and extracting tooth for histological analysis is no more necessary. With very high spatial resolution (~15 μm), OCT can increase the accuracy of diagnosis and the implementation of effective therapy to prevent secondary caries in dental clinics. The OCT images can reliably detect the location and dimension of microleakage. The calculated microleakage length was 401 μm and the width is 148 μm, which is consistent with the related histological biopsy measurements.

Conflict of Interests

The authors declare that there is no conflict of interests regarding the publication of this paper.

Acknowledgments

This work was supported in part by the Taiwan National Science Council under Grant nos. NSC 101-2628-E-009-026-MY3, NSC 102-2321-B-009-002, NSC 102-2622-E-009-007-CC3, NSC 102-2627-E-010-001, and NSC 102-3011-P-010-003 and a grant from Ministry of Education, Aim for the Top University Plan in National Chiao Tung University 101W9866.

References

[1] P. E. Petersen, *Future Use of Materials for Dental Restoration*, World Health Organization, Geneva, Switzerland, 2009.

[2] P. Timonen, M. Niskanen, L. Suominen-Taipale, A. Jula, M. Knuuttila, and P. Ylöstalo, "Metabolic syndrome, periodontal infection, and dental caries," *Journal of Dental Research*, vol. 89, no. 10, pp. 1068–1073, 2010.

[3] H. Akar, G. C. Akar, J. J. Carrero, P. Stenvinkel, and B. Lindholm, "Systemic consequences of poor oral health in chronic kidney disease patients," *Clinical Journal of the American Society of Nephrology*, vol. 6, no. 1, pp. 218–226, 2011.

[4] W. B. Grant, "A review of the role of solar ultraviolet-B irradiance and vitamin D in reducing risk of dental caries," *Dermato-Endocrinology*, vol. 3, no. 3, pp. 193–198, 2011.

[5] T. de Cássia Negrini, C. Duque, J. F. Höfling, and R. B. Gonçalves, "Fundamental mechanisms of immune response to oral bacteria and the main perspectives of a vaccine against dental caries: a brief review," *Journal of Dental Science*, vol. 24, no. 2, 2009.

[6] T. C. Paradella, F. A. C. G. de Sousa, C. Y. Koga-Ito, and A. O. C. Jorge, "Microbiological or chemical models of enamel secondary caries compared by polarized-light microscopy and energy dispersive X-ray spectroscopy," *Journal of Biomedical Materials Research Part B: Applied Biomaterials*, vol. 90B, no. 2, pp. 635–640, 2009.

[7] W. H. Arnold, T. Sonkol, A. Zoellner, and P. Gaengler, "Comparative study of in vitro caries-like lesions and natural caries lesions at crown margins: basic science research," *Journal of Prosthodontics*, vol. 16, no. 6, pp. 445–451, 2007.

[8] H. M. Nassar and C. González-Cabezas, "Effect of gap geometry on secondary caries wall lesion development," *Caries Research*, vol. 45, no. 4, pp. 346–352, 2011.

[9] A. Charuakkra, S. Prapayasatok, A. Janhom, S. Pongsiriwet, K. Verochana, and P. Mahasantipiya, "Diagnostic performance of cone-beam computed tomography on detection of mechanically-created artificial secondary caries," *Imaging Science in Dentistry*, vol. 41, no. 4, pp. 143–150, 2011.

[10] J. A. Rodrigues, K. W. Neuhaus, I. Hug, H. Stich, R. Seemann, and A. Lussi, "*In vitro* detection of secondary caries associated with composite restorations on approximal surfaces using laser fluorescence," *Operative Dentistry*, vol. 35, no. 5, pp. 564–571, 2010.

[11] D. Huang, E. A. Swanson, C. P. Lin et al., "Optical coherence tomography," *Science*, vol. 254, no. 5035, pp. 1178–1181, 1991.

[12] P. Wilder-Smith, K. Lee, S. Guo et al., "*In vivo* diagnosis of oral dysplasia and malignancy using optical coherence tomography: preliminary studies in 50 patients," *Lasers in Surgery and Medicine*, vol. 41, no. 5, pp. 353–357, 2009.

[13] M. Hangai, Y. Ojima, N. Gotoh et al., "Threedimensional imaging of macular holes with high speed optical coherence tomography," *Ophthalmology*, vol. 114, no. 4, pp. 763–773, 2007.

[14] M. C. Pierce, J. Strasswimmer, B. H. Park, B. Cense, and J. F. de Boer, "Birefringence measurements in human skin using polarization-sensitive optical coherence tomography," *Journal of Biomedical Optics*, vol. 9, no. 2, pp. 287–291, 2004.

[15] A. Baumgartner, S. Dichtl, C. K. Hitzenberger et al., "Polarization-sensitive optical coherence tomography of dental structures," *Caries Research*, vol. 34, no. 1, pp. 59–69, 2000.

[16] Y.-S. Hsieh, Y.-C. Ho, S.-Y. Lee et al., "Subgingival calculus imaging based on swept-source optical coherence tomography," *Journal of Biomedical Optics*, vol. 16, no. 7, Article ID 071409, 2011.

[17] M. A. Choma, M. V. Sarunic, C. Yang, and J. A. Izatt, "Sensitivity advantage of swept source and Fourier domain optical coherence tomography," *Optics Express*, vol. 11, no. 18, pp. 2183–2189, 2003.

[18] T. C. Paradella, C. Y. Koga-Ito, and A. O. C. Jorge, "Ability of different restorative materials to prevent in situ secondary caries: analysis by polarized light-microscopy and energy-dispersive X-ray," *European Journal of Oral Sciences*, vol. 116, no. 4, pp. 375–380, 2008.

[19] M. Bamzahim, A. Aljehani, and X.-Q. Shi, "Clinical performance of Diagnodent in the detection of secondary carious lesions," *Acta Odontologica Scandinavica*, vol. 63, no. 1, pp. 26–30, 2005.

[20] M. Bamzahim, X. Q. Shi, and B. Angmar-Månsson, "Secondary caries detection by DIAGNOdent and radiography: a comparative *in vitro* study," *Acta Odontologica Scandinavica*, vol. 62, no. 1, pp. 61–64, 2004.

[21] W. H. Arnold, T. Sonkol, A. Zoellner, and P. Gaengler, "Comparative study of *in vitro* caries-like lesions and natural caries lesions at crown margins: basic science research," *Journal of Prosthodontics*, vol. 16, no. 6, pp. 445–451, 2007.

[22] D. A. Cremersa and R. C. Chinnib, "Laser-induced breakdown spectroscopy—capabilities and limitation," *Applied Spectroscopy Reviews*, vol. 44, no. 6, pp. 457–506, 2009.

[23] P. H. P. D'Alpino, J. C. Pereira, N. R. Svizero, F. A. Rueggeberg, and D. H. Pashley, "Use of fluorescent compounds in assessing bonded resin-based restorations: a literature review," *Journal of Dentistry*, vol. 34, no. 9, pp. 623–634, 2006.

[24] I. Kanako, S. Yasushi, S. Alireza, S. Yasunori, and T. Junji, "Noninvasive cross-sectional visualization of enamel cracks by optical coherence tomography *in vitro*," *Journal of Endodontics*, vol. 38, no. 9, pp. 1269–1274, 2012.